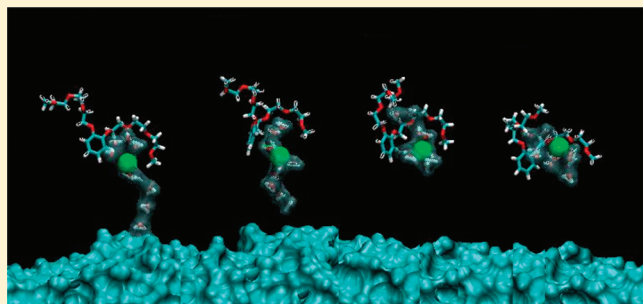


Transfer of the K⁺ Cation Across a Water/Dichloromethane Interface: A Steered Molecular Dynamics Study with Implications in Cation Extraction

Mário Valente, Sérgio Filipe Sousa, A. L. Magalhães,* and Cristina Freire*

REQUIMTE - Departamento de Química e Bioquímica, Faculdade de Ciências, Universidade do Porto, Rua Campo Alegre s/n, 4169-007, Porto, Portugal

ABSTRACT: In this paper we report the characterization of the dichloromethane (DCM)/water interface in terms of density profile, width, and surface structure. The use of steered molecular dynamics (SMD) to study the transfer of the K⁺ cation from the organic layer to the water layer is also described. The corresponding free energy is in semi-quantitative agreement with published experimental and theoretical results. The transference of the K⁺ cation from the water layer toward the DCM layer occurs with concomitant water transport as a water microdroplet that detaches itself from the water layer after ca. 16 Å of penetration into the organic layer by breaking the thin water thread that unites both. Complexation of the water microdroplet by a polyethylene-glycol type podand induces the loss of water molecules from the water microdroplet to bulk DCM and, eventually, to the water layer.



such as ours. Even more, SMD has been known to allow the study of rare events in a reasonable time span by application of a time dependent external force that pulls the system through a chosen reaction coordinate. An average of the work (W) done during this process over a set of transferences may be related to the free energy involved in the transference process (ΔG) by what is known as the Jarzynski identity¹⁰

$$\langle \exp[-W/k_B T] \rangle = \exp[-\Delta G/k_B T] \quad (1)$$

In fact, SMD has been used to get insights into processes such as the mechanical stability of proteins,^{11–19} the unfolding and the binding or unbinding of biomolecules,^{20–28} the transport across membranes,^{29–33} conformational studies,³⁴ the development of new materials,³⁵ the clarification of enzymatic pathways,³⁶ or the decomposition and complexation of alkali metal cations by a polyethylene-glycol type podand.³⁷ In this paper we report the use of SMD to assess the free energy involved in the K⁺ cation transfer from an organic (DCM) layer to an aqueous layer, as well as the free energy involved in the transfer (and water thread formation) of the K⁺ cation for the reverse process (from water toward the organic layer), and also to get insights on the active role played by an extraction agent [here a polyethylene-glycol type podand: 1,2-bis-{2-[2-(2-methoxy-ethoxy)-ethoxy]-ethoxy}-benzene, hereafter designated by b33 (Figure 1)] in what is usually known as assisted ion extraction.

Received: November 9, 2011

Revised: December 29, 2011

Published: January 19, 2012

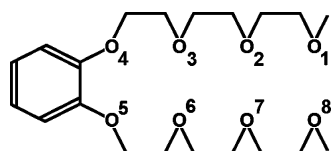


Figure 1. Schematic representation of the b33 podand and the oxygen atom numbering scheme used in the text.

METHODS

Molecular dynamics (MD) simulations were performed using the AMBER 9³⁸ software package. The b33 podand molecule was parametrized as previously described,^{39,40} in agreement with the typical premises followed in the general amber force field (GAFF).⁴¹ The van der Waals parameters used for the K⁺ cation were derived from the work of Åqvist,⁴² while DCM was accounted for using the molecular mechanics parameters of Fox and Kollman.⁴³ The water molecules were modeled by the well-known TIP3P model.⁴⁴ The present choices of molecular mechanics parameters and force field have been previously used with success in the study of metal podand interaction in water and/or dichloromethane systems.^{39,40}

Though very important in the study of the dipole variation across interfaces and the interaction between ions and solvent molecules, the use of nonpolarizable models seems to be a minor drawback.^{45–47} A note must also be introduced here about our choice of force field: It is well-known that while other (more recent) force fields are nowadays available their increased parametrization complexity does not necessarily offer an increase in phenomenological validity over the well tested and here used force field, whereas the increase in processor time may be considerable.

The working double solvent (dichloromethane/water) box was built from a starting assembly of 692 DCM and 1815 water molecules in a square prismatic box of 74 × 45 × 45 Å (*x,y,z*). An initial ten thousand steps minimization stage was performed on this box by applying the steepest descent method followed by an equal number of steps using the conjugate gradient method. This minimization was followed by an equilibration stage performed sequentially in two moments: to begin with, the systems were allowed to heat from 0 to 300 K in fifty thousand steps (with a time step of 1 fs), corresponding to 50 ps, using temperature control (Langevin dynamics with 1 ps⁻¹ collision frequency), at constant volume (no pressure controls were applied). In the second equilibration step the system was allowed to run for one million steps, corresponding to 1 ns, at 300 K, using the same temperature control conditions, at constant (isotropic) pressure, with a pressure relaxation time of 2 ps, in order to achieve the proper final density. The final box dimensions (*x,y,z*) are 63 × 38 × 38 Å.

A 1 ns production step was run on the resulting double solvent box, in order to characterize the water/DCM interface. The conditions used for this production step were the same as the ones used in the second equilibration step. During this production run information was extracted at a 200 step frequency, generating five thousand frames. Throughout all minimization, equilibration and production steps a cutoff value of 12 Å was used for the treatment of the nonbonded interactions.

The systems to be used in the steered molecular dynamics (SMD) runs designed to study the transference of a K⁺ cation across the water/DCM interface were prepared by immersing the cation into the center of the bulk organic phase (or the

water phase), followed by a minimization step as described above, and an equilibration step using the same conditions as already described but with a duration of 250 ps, which was found to be enough to achieve a constant total density. During this equilibration step the K⁺ cation was kept in place by applying a restraining force constant (200 kcal mol⁻¹ Å⁻²).

For the experiments involving the crossing of the K⁺ cation through the interface, the target atoms for the SMD runs (the oxygen atoms of selected water molecules or the carbon atoms of selected DCM molecules) were chosen from the corresponding last equilibration frame (also used as the starting frame in the production runs). During the SMD runs the movements of these target atoms were restrained by application of a force constant of 200 kcal mol⁻¹ Å⁻². The K⁺ cation was kept at his target-approach trajectory by a force constant of 50 kcal mol⁻¹ Å⁻², using the same conditions as for the production runs. The chosen total time of 1 ns roughly corresponds to a mean velocity of 0.05 Å ps⁻¹ which is a common choice for alkali cations in water⁴⁸ (and should also be enough for DCM as it is a less viscous solvent than water), thus effectively minimizing unnatural friction effects with the solvent that may result in considerable nonconservative work.

In the complexation studies involving the b33 podand in the organic phase, the molecule was immersed in bulk DCM and equivalent minimization and equilibration steps as described above were performed while keeping the solute in the center of the DCM phase, by use of a force constant of 200 kcal mol⁻¹ Å⁻² applied on a carbon atom of the aromatic ring and allowing the rest of the molecule to adjust to the solvent. In the subsequent SMD runs, the podand molecule (as well as a nearby DCM molecule: the target) was kept near the center of the DCM phase (at ca. 20 Å from the water layer), again by applying a force constant of 200 kcal mol⁻¹ Å⁻² on a carbon atom of the aromatic ring (and the central carbon atom of the DCM molecule) while allowing the rest of the molecule to adjust to the solvent.

All supporting quantum calculations presented below were performed at the HF/6-31G(d) level of theory for consistency reasons with our choice of force field,⁴¹ using the Gaussian 03 package.⁴⁹

RESULTS AND DISCUSSION

Water/DCM Interface. A 1 ns MD production run was performed on the above characterized double solvent box in order to characterize the resulting interface unperturbed by the presence of a solute. Analysis of the resulting MD trajectories is described in the following paragraphs.

By taking into consideration the number of the DCM carbon atoms as well as number of water oxygen atoms present in slabs (with a resolution of 1 Å) parallel to the interfacial plane for the whole double-solvent box we were able to build the longitudinal (*x* axis) mean density profile (Figure 2). This density profile was adjusted to the following expression, proposed by Matsumoto and Kataoka:⁵⁰

$$\rho(x) = \frac{1}{2}(\rho_{DCM} + \rho_{WAT}) - \frac{1}{2}(\rho_{DCM} - \rho_{WAT}) \tanh((x - x_{GDS})/d) \quad (2)$$

where ρ_{DCM} and ρ_{WAT} are the DCM and water densities, respectively, x_{GDS} is the *x* position of the Gibbs dividing surface (GDS; a geometrical surface that marks the point where the density of each solvent is half its bulk value), and *d* is the

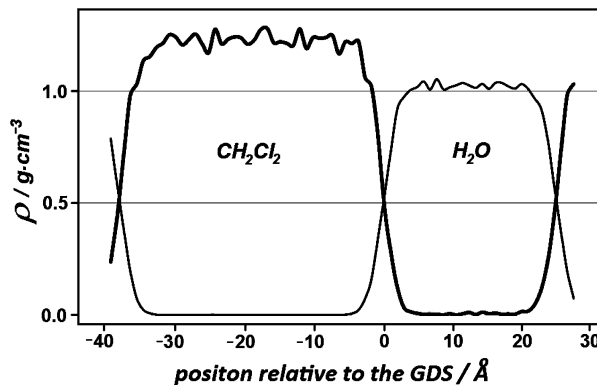


Figure 2. Longitudinal (x axis) mean density (ρ) profile of the double solvent box (dichloromethane, thick line; water, narrow line).

interfacial width. The resulting adjustment allowed us to estimate an interfacial width of 2.30 \AA , which is in reasonable accord with the result previously determined by Dang⁵ (of 2.37 \AA) for the same double-solvent system, using a polarizable model for water and for DCM.

The so-called “10–90” thicknesses (as defined by Matsumoto and Kataoka⁵⁰) found for our system were 4.7 \AA and 5.1 \AA for DCM and water at the interface, respectively. These values are somewhat higher than those found by Dang⁵ (4.1 \AA and 4.6 \AA). The differences found are probably due to the use of polarizable models for the water and the DCM molecules, by Dang, whereas our models are nonpolarizable.

The bulk density values found for both solvents (1.02 g/cm^3 for water and 1.23 g/cm^3 for DCM) are very similar to the ones found for the same system by Hantal and co-workers⁸ (1.00 g/cm^3 for water and 1.20 g/cm^3 for DCM) and are also near to the experimental ones (1.00 g/cm^3 for water and 1.32 g/cm^3 for DCM).

The water-DCM interfacial width of 2.30 \AA is considerably lower than the (water) oxygen–(DCM) carbon distance of 3.23 \AA found for the quantum calculated optimized structure of the $\text{H}_2\text{O}-\text{CH}_2\text{Cl}_2$ dimer, which is in agreement with what is reported in other studies where sharp but irregular molecular arrangements at the interface were found,^{51–54} due to the occurrence of low frequency capillary waves (corresponding to an effective solvent interpenetration forming the so-called “solvent fingers”) that result in the overall contraction of the interfacial width.⁵⁴

SMD Guided Transferences of K across the Interface.

In the following paragraphs a phenomenological description of the transference of the K^+ cation from DCM to water and from water to DCM is made. In the latter case, the formation of water threads is described. The free energy values for the DCM-to-water transference and for the formation of the water thread are determined by use of the Jarzinski equality.

While considering the K^+ transference from the bulk DCM phase to the bulk water phase, we noticed that the cation is not accompanied by DCM molecules, and there is not even a significant penetration of the organic molecules into the aqueous layer at the point where the K^+ cation crosses the interface.

Again, according to the Jarzynski equality, the free energy involved in the transference of the K^+ cation from the bulk DCM phase to the bulk water phase is equivalent to the average of the work done during the process by an applied external force in a series of simulations (Figure 3). The free energy

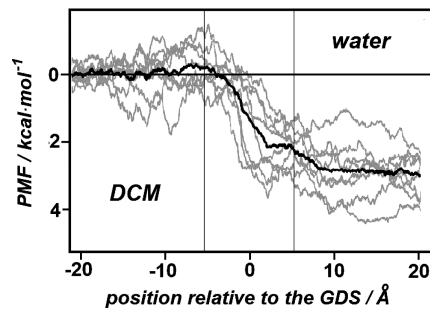


Figure 3. Plots of the work (PMF) executed along the reaction coordinate (the pulling of a K^+ cation from bulk DCM to bulk water) for various SMD runs (light gray lines) and their corresponding mean (black line). Vertical lines are presented at $\pm 5 \text{ \AA}$ of the GDS for comparison purposes.

determined was $-3 \pm 1 \text{ kcal mol}^{-1}$ (based on ten independent SMD experiments, $n = 10$), a considerably lower value (in absolute terms) than the experimental one of $-7.68 \text{ kcal mol}^{-1}$ but closer to the theoretical value of $-6.4 \text{ kcal mol}^{-1}$ determined by Abraham and Liszi⁵⁵ and even closer to the calculated value of $-4.7 \pm 0.4 \text{ kcal mol}^{-1}$ using the equation proposed by Abraham and Acree.⁵⁶ A plausible reason for the difference between the SMD determined value and the experimental and theoretical values reported resides in the use of a nonpolarizable force field that results in a lower stabilization of the cation in water and, thus, a slightly lower (in absolute terms) estimated free energy value for the transference process across the interface. Nonetheless, the (small) negative free energy value estimated supports the experimental observation that there is a tendency for the K^+ cation to transfer spontaneously from DCM to water.

A typical plot of the K^+ cation position on the X axis as a function of simulation time for the transference from the organic layer to the aqueous layer (Figure 4A) shows that the

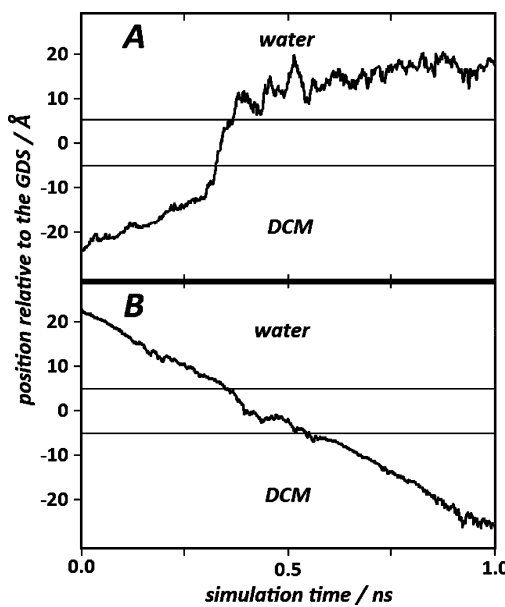


Figure 4. Typical plots of the position of the K^+ cation relative to the GDS as a function of the simulation time for (A) the transference from DCM to water and (B) the transference from water to DCM. Horizontal lines are presented at $\pm 5 \text{ \AA}$ of the GDS for comparison purposes.

cation considerably increases its velocity toward the aqueous phase ca. 10 Å before it reaches the GDS, showing the importance of long-range interactions in this process (one must notice that the cutoff value used was 12 Å). A similar observation was already made by Benjamin.⁵⁷

In the forced transference of K⁺ from the water phase to the DCM phase the cation is always accompanied by water molecules that initially form threads that protrude up to a maximum length of about 16 Å ($n = 6$) into the organic layer. These threads eventually break thus leaving a water microdroplet (containing 7 to 12 water molecules) surrounding the K⁺ cation in bulk DCM (Figure 5).

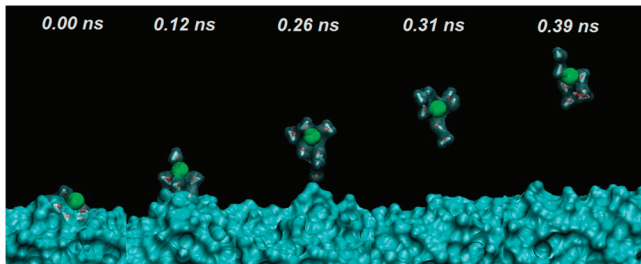


Figure 5. Sequential representation of selected frames showing the pulling of the K⁺ cation (immersed in a water microdroplet containing seven water molecules) from bulk water into bulk DCM, during a typical SMD run. The time values shown on top are relative to the emergence of the K⁺ cation from the water layer.

This cotransport of water molecules may be seen as the ionic correspondent to the “water dragging” effect shown by organic molecules while crossing water–organic solvent interfaces.^{58,59}

Using the above-mentioned Jarzynski equality, the free energy involved in the protrusion of the K⁺ containing water threads is equivalent to the mean of the work done during the pulling or the K⁺ cation (until the thread breaks) by an applied external force in a series of simulations (Figure 5). After subtraction of the K⁺ cation transference free energy (3 kcal mol⁻¹) the calculated mean free energy of water finger formation is 34 ± 3 kcal mol⁻¹ ($n = 10$) corresponding to a free energy of water finger growth of 2.3 kcal mol⁻¹ Å⁻¹.

A typical plot of the K⁺ cation position on the X axis as a function of simulation time for the transference from the aqueous layer to the organic layer (Figure 4B) shows that on contact with the GDS the cation lowers its velocity toward the organic phase, showing strong close range repulsive interactions in this particular process. After crossing the GDS the velocity is again constant, even though the pulling force is now creating a water thread.

It is interesting to note in Figures 3, 4, and 6, as mentioned by Benjamin,⁵⁷ that the free energy profiles show that the K⁺ ion begins to feel the surface when it is about 8 Å away from the GDS.

Complexation in the Organic Phase. In order to get some insights into the complexation of the K⁺ cation containing water microdroplet SMD simulations were carried out on systems consisting of a b33 podand molecule in the bulk organic phase and a K⁺ cation in the bulk aqueous phase. In the starting SMD run the cation was pulled from its initial location, across the interface, toward the podand. Then a sequence of MD runs was performed (for a total time of 7 ns) in order to follow the loss of water molecules by the complex formed between the water microdroplet, the K⁺ cation and the b33

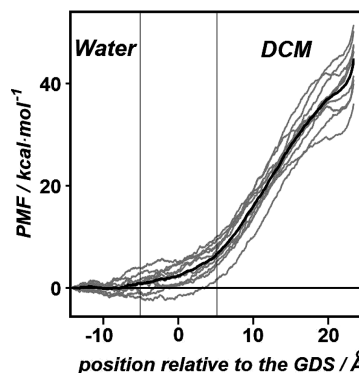


Figure 6. Plots of the work (PMF) executed along the reaction coordinate (the pulling of a K⁺ cation and water thread from bulk water to bulk DCM) for various SMD runs (light gray lines) and their corresponding mean (black line). Vertical lines are presented at ±5 Å of the GDS for comparison purposes.

podand. It was found that loss of water molecules occurs haphazardly at a low rate (usually one molecule per ca. 1.5 ns) or in group (usually two to four molecules) when spontaneously formed water threads reconnect with the water phase and break (with global loss of water molecules).

In the course of our MD simulations, the podand was able to quickly break the water thread (Figure 7) and complex the K⁺

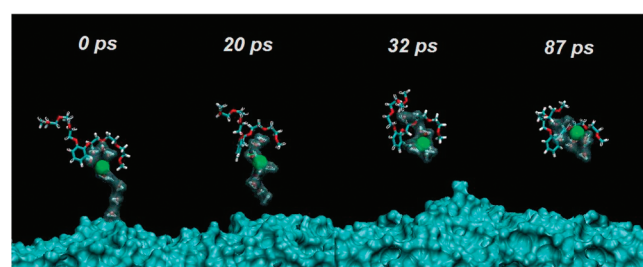


Figure 7. Sequential representation of selected frames showing the complexation of a water microdroplet (containing a K⁺ cation and nine water molecules) by the b33 podand. The time values shown on top are relative to the beginning of a free MD run performed after the SMD run that pulled the cation out of the water layer.

cation, either directly or indirectly by establishing hydrogen bonds with water molecules that in turn directly interact with the cation (Figure 8). This creates a complex web of interactions that effectively fixes the cation to the podand, as already described before.⁴⁰

Single-point quantum calculations performed on five stochastically chosen complex structures (comprising the cation, the b33 podand molecule and eight water molecules) from the MD simulations allowed the counterpoise corrected estimation of the interaction energies between the cation and the b33 podand (−42 ± 6 kcal mol⁻¹), corresponding to a stabilizing interaction between the cation and ca. three podand oxygen atoms, and between the cation and the water microdroplet (−67 ± 3 kcal mol⁻¹) but a slightly destabilizing interaction between the b33 podand and the water microdroplet (7 ± 7 kcal mol⁻¹). These results point to a stronger stabilization of the cation by the water microdroplet when compared to its stabilization by the b33 podand, but to an even stronger cation stabilization by the b33 podand and the water microdroplet combined. This provides an explanation of the

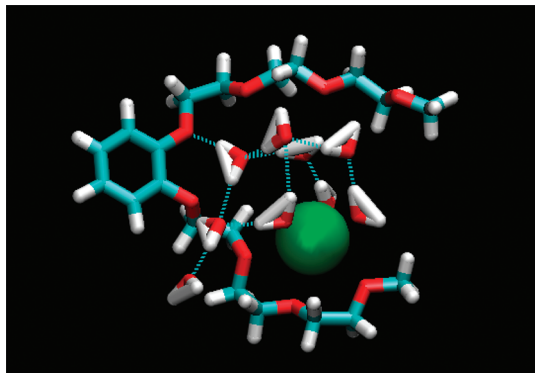


Figure 8. Schematic representation of a typical frame of the complex formed between the b33 podand and a microdroplet (containing the K^+ cation and nine water molecules) in bulk DCM. The light-blue dashed lines indicate a highly structured set of hydrogen bonds.⁵⁸

reason why the cation is extracted to the organic phase in the presence of a b33 podand molecule.

In fact, as the complex was kept at ca. 20 Å from the aqueous layer, gradually, water molecules were lost. This happened in two different ways: (i) a spontaneous and rare (as it only happened once in the 5 ns of simulation time) unimolecular loss (Figure 9, 0.90 ns) or (ii) a water thread formation with

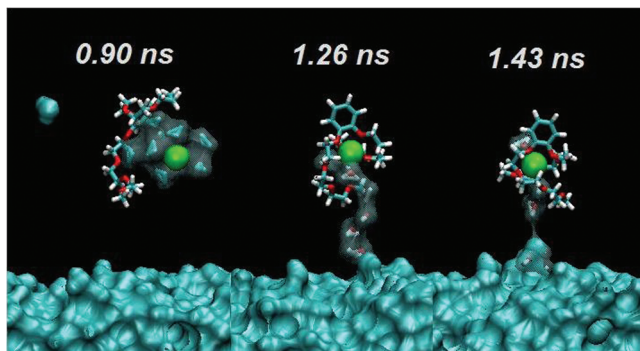


Figure 9. Selected frames showing loss of water molecules by the b33 complexed, K^+ cation containing, water microdroplet. The time values shown on top are relative to the beginning of a free MD run performed after the SMD run that pulled the cation out of the water layer.

direct loss to the water layer (Figure 9, 1.26 and 1.43 ns). The first way occurred when small water threads formed⁴⁰ and the outmost water molecule “lost its grip” of the other water molecules and migrated to bulk DCM and eventually into the water layer. The second way happened when a water thread connected with the water layer and simply broke with the concomitant loss of water molecules that quickly reintegrated the water layer. In fact, as the simulation evolved, while the K^+ cation established strong interactions with an increasing number of podand oxygen atoms, the released water molecules were able to form longer (and less stable) water threads that strongly contributed to a quicker water loss.

After 5 ns of MD the initial complex had lost all but two of the original water molecules and gained one water molecule that was spontaneously released from the water layer.

Again, single-point quantum calculations performed on five stochastically chosen complex structures (comprising the cation, the b33 podand molecule and three water molecules)

from the MD simulations allowed the counterpoise corrected estimation of the interaction energies between the cation and the b33 podand (-81 ± 7 kcal mol⁻¹), corresponding to attractive interactions between the cation and the eight podand oxygen atoms, between the cation and the water microdroplet (-27 ± 4 kcal mol⁻¹) and repulsive interactions between the b33 podand and the water microdroplet (13 ± 2 kcal mol⁻¹). At this stage of the transference, there is a stronger stabilization of the cation by the b33 podand when compared to its stabilization by the water microdroplet. The stronger destabilizing interaction between the b33 podand and the water microdroplet may explain the gradual loss of water molecules by the complex as with fewer water molecules interacting with the cation none will form hydrogen bonds with the podand oxygen atoms (Figure 10) and, as such, there will

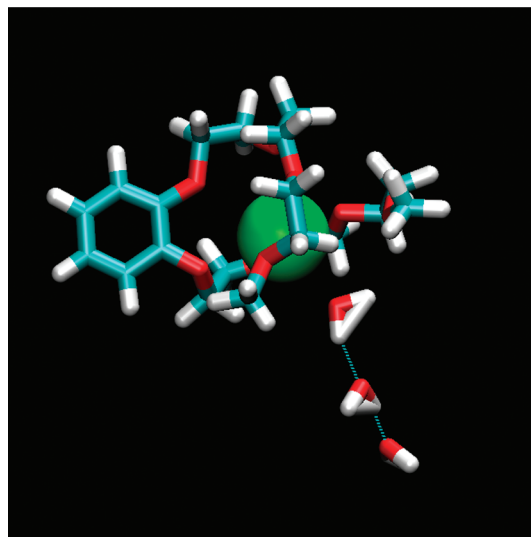


Figure 10. Schematic representation of a typical frame of the complex formed between the b33 podand and a microdroplet (containing the K^+ cation and three water molecules) in bulk DCM. The light-blue dashed lines represent the hydrogen bonds.⁵⁸

be a destabilizing dipolar interaction between the water molecules and the cavity created by the b33 podand to accommodate the cation.

These results seem to indicate that after transference from the water layer to the organic layer the K^+ complex gradually loses its hydration sphere in a process where the extraction agent (and surely bulky anions as the picrate) plays an important role, by weakening the K^+ cation–water interactions and by surrounding the cation and, at the end, possibly more or less effectively protecting it from interacting with extra water molecules. To some degree the above-mentioned results concur with what has already been suggested by Chorny and Benjamin,⁶¹ that for a water molecule to leave the hydration shell in a region where few water molecules exist (as in bulk DCM) it must find a hydrogen-bonding partner (here the b33 podand). Another cause for the partial loss of the hydration shell hinted by our results derives from the repulsive interaction between the podand and the water molecules, in particular when the podand is effectively wrapped around the cation.

CONCLUSIONS

The SMD results for the free energy involved in the K^+ cation transference across the DCM–water interface are somewhat low

(in absolute terms) when compared with other experimental and theoretical ones, but all point to a spontaneous crossing of the interface toward the water phase. The K^+ cation transference from water to DCM is accompanied by a water dragging effect, where the cation is surrounded by a water microdroplet containing up to twelve water molecules. This water droplet remains linked to the aqueous phase by a water thread of up to 16 Å in length and one molecule in width, after which it breaks. The estimated water thread formation free energy is 34 ± 3 kcal mol⁻¹, i.e., of about 2 kcal mol⁻¹ per Å.

The transference of a K^+ cation from water to DCM is energetically hindered but the simple presence of an extraction agent (here a polyethylene-glycol type podand, b33) seems to be able to stabilize the cation in bulk DCM by first establishing weak hydrogen bonds with the water molecules that constitute the water microdroplet surrounding the cation and a few stronger (up to three) interactions directly with the cation. After gradual loss of most water molecules, in about 2–3 ns (due to destabilizing water-podand interactions), i.e., after almost complete substitution of the first hydration sphere, the podand is mostly wrapped around the cation. Nonetheless, up to three water molecules continue linked to the cation in the complex after 5 ns of simulation time.

Further studies involving other cations are in course, in order to clarify the experimentally found extraction selectivity.

AUTHOR INFORMATION

Corresponding Author

*E-mail: almagalh@fc.up.pt; acfreire@fc.up.pt.

ACKNOWLEDGMENTS

This work has been supported by Fundação para a Ciência e a Tecnologia through Grant No. Pest-C/EQB/LA0006/2011.

REFERENCES

- (1) Chang, T.-M.; Dang, L. X. *Chem. Rev.* **2006**, *106*, 1350–1322.
- (2) de Namor, A. F. D.; Traboulssi, R.; Salazar, F. F.; de Acosta, V. D.; de Vizcardo, Y. F.; Portugal, J. M. *J. Chem. Soc. Faraday Trans. 1* **1989**, *85*, 2705–2712.
- (3) de Namor, A. F. D.; Pugliese, A.; Casal, A. R.; Llerena, M. B.; Aymonino, P. J.; Velarde, F. J. *S. Phys. Chem. Chem. Phys.* **2000**, *2*, 4355–4360.
- (4) Valente, M.; Sousa, S. F.; Magalhães, A. L.; Freire, C. *J. Sol. Chem.* **2010**, *39*, 1230–1242.
- (5) Dang, L. X. *J. Chem. Phys.* **1999**, *110*, 10113–10122.
- (6) Dang, L. X. *J. Phys. Chem. B* **2001**, *105*, 804–809.
- (7) Hore, D. K.; Walker, D. S.; MacKinnon, L.; Richmond, G. L. *J. Phys. Chem. C* **2007**, *111*, 8832–8842.
- (8) Hantal, G.; Terleczky, P.; Horvai, G.; Nyulászi, L.; Jedlovszky, P. *J. Phys. Chem. C* **2009**, *113*, 19263–19276.
- (9) van Gunsteren, W. F.; Mark, A. E. *J. Chem. Phys.* **1998**, *108*, 6109–6116.
- (10) Jarzynski, C. *Phys. Rev. Lett.* **1977**, *78*, 2690–2693.
- (11) Duzman, D. L.; Randal, A.; Baldi, P.; Guan, Z., *Proc. Natl. Acad. Sci.* **2011**, www.pnas.org/cgi/doi/10.1073/pnas.0905796107
- (12) Lu, H.; Izraelewitz, B.; Krammer, A.; Vogel, V.; Shulten, K. *Biophys. J.* **1998**, *75*, 662–671.
- (13) Pappalardo, M.; Milardi, D.; Grasso, D.; La Rosa, C. *New. J. Chem.* **2007**, *31*, 901–905.
- (14) Ozer, G.; Valeev, E. F.; Quirk, S.; Hernandez, R. *J. Chem. Theory Comput.* **2010**, *6*, 3026–3038.
- (15) Ho, B. K.; Agard, D. A. *PLoS ONE* **2010**, *5*, e13068.
- (16) Park, S.; Shulten, K. *J. Chem. Phys.* **2004**, *120*, 5946–5961.
- (17) Hummer, G.; Szabo, A. *Biophys. J.* **2003**, *85*, 5–15.
- (18) Hummer, G.; Szabo, A. *Proc. Natl. Acad. Sci.* **2001**, *98*, 3658–3661.
- (19) Liu, X.; Xu, Y.; Wang, X.; Barrantes, F. J.; Jiang, H. *J. Phys. Chem. B* **2008**, *112*, 4087–4093.
- (20) Niu, C.; Xu, Y.; Luo, X.; Duan, W.; Silman, I.; Sussman, J. L.; Zhu, W.; Chen, K.; Shen, J.; Jiang, H. *J. Phys. Chem. B* **2005**, *109*, 23730–23738.
- (21) Caballero, J.; Zamora, C.; Aguayo, D.; Yañez, C.; González-Nilo, F. D. *J. Phys. Chem. B* **2008**, *112*, 10194–10201.
- (22) Martínez, L.; Polycarpov, I.; Skaf, M. S. *J. Phys. Chem. B* **2008**, *112*, 10741–10751.
- (23) Yang, L.-J.; Zou, J.; Xie, H. Z.; Li, L.-L.; Wei, Y.-Q.; Yang, S.-Y. *PLoS ONE* **2009**, *4*, e8470.
- (24) Hanasaki, I.; Haga, T.; Kawano, S. *J. Phys.: Condens. Matter* **2008**, *20*, 255238–255248.
- (25) Yechun, X.; Jianhua, S.; Xiaomin, L.; Xu, S.; Kaixian, C.; Hualiang, J. *Sci. Chin. B Chem.* **2004**, *47*, 355–366.
- (26) Orzechowski, M.; Cieplak, P. *J. Phys.: Condens. Matter* **2005**, *17*, S1627–S1640.
- (27) Amaro, R.; Tajkhorssig, E.; Luthey-Shulthen, Z. *Proc. Natl. Acad. Sci.* **2003**, *100*, 7599–7604.
- (28) Bizzarri, A. R. *J. Phys. Chem. B* **2011**, *115*, 1211–1219.
- (29) Tepper, H. L.; Voth, G. A. *J. Phys. Chem. B* **2006**, *110*, 21327–21337.
- (30) Liu, Z.; Xu, Y.; Tang, P. *J. Phys. Chem. B* **2006**, *110*, 12789–12795.
- (31) Jensen, M. Ø.; Park, S.; Tajkhorshid, E.; Shulten, K. *Proc. Natl. Acad. Sci.* **2002**, *99*, 6731–6736.
- (32) Monticelli, L.; Robertson, K. M.; MacCallum, J. L.; Tielemans, D. P. *FEBS Lett.* **2004**, *564*, 325–332.
- (33) Saito, H.; Shinoda, W. *J. Phys. Chem. B* **2011**, *115*, 15241–15250.
- (34) Wu, X.; Wang, S. *J. Phys. Chem. B* **1998**, *102*, 7238–7250.
- (35) Guzmán, D. L.; Roland, J. T.; Keer, H.; Kong, Y. P.; Ritz, T.; Yee, A.; Guan, Z. *Polymer* **2008**, *49*, 3892–3901.
- (36) Crespo, A.; Martí, M. A.; Estrín, D. A.; Roitberg, A. E. *J. Am. Chem. Soc.* **2005**, *127*, 6940–6941.
- (37) Valente, M.; Sousa, S. F.; Magalhães, A. L.; Freire, C. *Theor. Chem. Acc.* accepted.
- (38) Case, D. A.; Darden, T.; Cheatham, T.; Simmerling, C. L.; Wang, J.; Duke, R. E.; Luo, R.; Merz, K. M.; Perlman, D. A.; Crowley, M.; et al. *AMBER 9*; University of California: San Francisco, CA, 2006.
- (39) Valente, M.; Sousa, S. F.; Magalhães, A. L.; Freire, C. *J. Molec. Struct. TEOCHEM* **2010**, *946*, 77–82.
- (40) Valente, M.; Sousa, S. F.; Magalhães, A. L.; Freire, C. *Theor. Chem. Acc.* **2010**, *127*, 681–687.
- (41) Wang, J.; Wolf, R. M.; Caldwell, J. W.; Kollman, P. A.; Case, D. A. *J. Comput. Chem.* **2004**, *25*, 1157–1174.
- (42) Åqvist, J. *J. Phys. Chem.* **1990**, *94*, 8021–8024.
- (43) Fox, T.; Kollman, P. A. *J. Phys. Chem. B* **1998**, *102*, 8070–8079.
- (44) Jorgensen, W. L.; Chandrasekhar, J.; Madura, J. D.; Impey, R. W.; Klein, M. L. *J. Chem. Phys.* **1983**, *79*, 926–936.
- (45) Matababir, K. A.; Berkowitz, M. L. *Chem. Phys. Lett.* **2006**, *176*, 61–66.
- (46) Dang, L. X.; Chang, T.-M. *J. Phys. Chem. B* **2002**, *106*, 235–238.
- (47) Sieffert, N.; Chaumont, A.; Wipff, G. *J. Phys. Chem. C* **2009**, *113*, 10610–10622.
- (48) Cascella, M.; Guidoni, L.; Maritan, A.; Rothlisberger, U.; Carloni, P. *J. Phys. Chem. B* **2002**, *106*, 13027–13032.
- (49) Frisch, M. J.; et al. *Gaussian 03*, revision C.02; Gaussian Inc.: Wallingford, CT, 2004.
- (50) Matsumoto, M.; Kataoka, Y. *J. Chem. Phys.* **1988**, *88*, 3233–3245.
- (51) Benjamin, I. *Chem. Phys. Lett.* **2009**, *469*, 229–241.
- (52) Muzet, N.; Enler, E.; Wipff, G. *J. Phys. Chem. B* **1998**, *102*, 10772–10788.
- (53) Varnek, A.; Troxler, L.; Wipff, G. *Chem.—Eur. J.* **1997**, *3*, 552–560 and references therein.

- (54) Zhang, Y.; Feller, S. E.; Brooks, B. R.; Pastor, R. W. *J. Chem. Phys.* **1995**, *103*, 10252–10266.
- (55) Abrahams, M. H.; Liszi, J. *J. Inorg. Nucl. Chem.* **1981**, *43*, 143–151.
- (56) Abrahams, M. H.; Acree, W. E. *J. Org. Chem.* **2010**, *75*, 1006–1015.
- (57) Benjamin, I. *Chem. Rev.* **1996**, *96*, 1449–1475.
- (58) Tsai, R.-S.; Fan, W.; El Tayar, N.; Carrupt, P.-A.; Testa, B.; Kier, L. B. *J. Am. Chem. Soc.* **1993**, *115*, 9632–9639.
- (59) Fan, W.; Tsai, R.-S.; El Tayar, N.; Carrupt, P.-A.; Testa, B. *J. Phys. Chem.* **1994**, *98*, 329–333.
- (60) The hydrogen bonds here presented obey the usual criteria ($R < 3.5 \text{ \AA}$ and $\Theta < 30^\circ$) as in Laage, D.; Hynes, J. T. *Science* **2006**, *311*, 832–835.
- (61) Chorny, I.; Benjamin, I. *J. Phys. Chem. B* **2005**, *109*, 16455–16462.